Campbell, I. D., Dobson, C., & Williams, R. J. P. (1975a) *Proc. R. Soc. London, B 189*, 485–502.
Campbell, I. D., Dobson, C., & Williams, R. J. P. (1975b) *Proc. R. Soc. London, B 189*, 503–517.
Campbell, I. D., Dobson, C., & Williams, R. J. P. (1975c) *Proc. R. Soc. London, A 345*, 23–40.
Campbell, I. D., Dobson, C., & Williams, R. J. P. (1975d) *Proc. R. Soc. London, A 345*, 41–59.
Dubs, A., Wagner, G., & Wüthrich, K. (1979) *Biochim. Biophys. Acta 577*, 177–194.
Esch, F. S., Bohlen, P., Otsuka, A. A., Yoshida, M., & Allison, W. S. (1981) *J. Biol. Chem. 256*, 9084–9089.
Frasch, W. D., & Selman, B. (1981) *Biochemistry 20*, 3636–3643.
Frasch, W. D., & Sharp, R. R. (1984) *Adv. Photosynth. Res., Proc. Int. Congr. Photosynth., 6th 2*, 591–594.
Frasch, W. D., & Sharp, R. R. (1985) *Biochemistry* (following paper in this issue).
Lindon, J. C., & Ferrige, A. G. (1979) *J. Magn. Reson. 36*, 277–280.
Moroney, J. V., Lopresti, L., McEwen, B. F., McCarty, R. E., & Hammes, G. G. (1983) *FEBS Lett. 158*, 58–62.
Nelson, N. (1981) *Curr. Top. Bioenerg. 11*, 1–29.
Wagner, G., & Wüthrich, K. (1982) *J. Mol. Biol. 155*, 347–366.
Wider, G., Lee, K. H., & Wüthrich, K. (1982) *J. Mol. Biol. 155*, 367–388.
Wüthrich, K. (1980) *Front. Bioorg. Chem. Mol. Biol., Proc. Int. Symp.*, 161–168.
Wüthrich, K. (1981) *Macromol. Chem. Phys., Suppl. No. 5*, 234–252.
Wüthrich, K. (1983) *Biopolymers 22*, 131–128.

Nucleotide Binding to Chloroplast ATP Synthase: Effect on the Proton Spin-Echo NMR Spectrum†

W. D. Frasch*,‡ and R. R. Sharp§

Department of Cellular and Molecular Biology and Department of Chemistry, The University of Michigan, Ann Arbor, Michigan 48109

Received January 4, 1985

ABSTRACT: Effects of nucleotide binding on the high-resolution proton spin-echo spectrum of chloroplast ATP synthase [coupling factor 1 (CF_1)] have been studied. Spin-echo difference spectra obtained at an 18-ms pulse spacing have been recorded ± stoichiometric amounts of 5′-adenylyl β-imidodiphosphate (AMPPNP), a nonhydrolyzable substrate analogue. Addition of Mg·AMPPNP to solutions of CF_1 causes a highly specific shortening of T_2 of two proton resonances at 2.70 and 2.29 ppm, which have previously been assigned to β- and γ-methylene protons of aspartate and glutamate, respectively, on the basis of studies of the effects of covalent modification of carboxyl-bearing side chains on CF_1. The observed T_2 shortening, which indicates decreased mobility of these side chains in the presence of nucleotide, results from nucleotide binding to a tight side ($K_d \approx 10^{-6}$ M) which is present at a mole ratio of 1 mol of nucleotide per mole of CF_1. Parallel experiments have also been conducted with the mangano-AMPPNP complex, which is paramagnetic and can produce additional relaxation enhancements of neighboring protons by means of the through-space nuclear dipole–electron dipole interaction. The effective range of this interaction in the present experiments is estimated to be at least 19 Å but no greater than 25 Å. From a comparison of relaxation enhancements produced by Mg·AMPPNP with those produced by Mn·AMPPNP, it is concluded that the majority of the resonances visible in the 18-ms spin-echo NMR spectrum lie outside the dipolar sphere of influence. The aspartate and glutamate resonances which are immobilized by Mg·AMPPNP binding do not coordinate directly to the metal ion but lie near the periphery of this sphere.

Coupling factor 1 (CF_1)[1] is the extrinsic membrane protein complex which contains the active site of the proton-translocating ATP synthase of the chloroplast thylakoid membrane. This enzyme mediates the transfer of free energy from the protonmotive force produced by photosynthetic electron transport to the synthesis of the terminal phosphate bond of ATP. CF_1 is composed of five distinct subunits, the apparent stoichiometry of which is $\alpha_3, \beta_3, \gamma, \delta, \epsilon$ (Dunn & Hepple, 1981; Penefsky, 1979; Merchant et al., 1983). The overall molecular weight of the extrinsic protein complex is 400K–407K (Moroney et al., 1983). Evidence suggesting that the site of ATP synthesis resides on the β subunit (Carlier et al., 1979) supports the presence of three catalytic sites per CF_1 (Moroney et al., 1983). Substrate binding at the three active sites is believed to be strongly coupled during the catalytic cycle (Boyer, 1980).

Catalysis appears to involve an S_N2 mechanism (Webb, 1980), and the active conformation of the substrate is known to be a Λ-bidentate nucleotide complex with a divalent metal cation (Frasch & Selman, 1981). The active site also dem-

† This work was supported by grants from the U.S. Department of Agriculture (83-CRCR-1-1339) to W.D.F. and R.R.S. and from the Rackham Foundation and the Phoenix Memorial Research Foundation to W.D.F.

‡ Department of Cellular and Molecular Biology.
§ Department of Chemistry.

[1] Abbreviations: AMPPNP, 5′-adenylyl β-imidodiphosphate; SE, spin-echo; SED, spin-echo difference; CF_1, chloroplast coupling factor 1; DTT, dithiothreitol; WRK, Woodward's reagent K (*N*-ethyl-5-phenylisoxazolium-3′-sulfonate); DCCD, dicyclohexylcarbodiimide.

0006-2960/85/0424-5454$01.50/0

onstrates stereospecificity for the trans–gauche–gauche configuration of the ribose of the nucleotide (Schlimme et al., 1979). Structural information concerning the identity of amino acids involved in substrate binding has been based primarily on studies in which covalent modification of specific amino acids inactivates the enzyme in a manner that can be prevented by the presence of substrate (Vallehos, 1981). Covalent modification studies of CF_1 have implicated several charged or polar amino acids at the active site. These amino acids include tyrosine (Deters et al., 1975; Cantley & Hammes, 1975), arginine (Schmid et al., 1977; Vallejos et al., 1977), lysine (Oliver & Jagendorf, 1976; Sugayama & Mukohata, 1978, 1979), and at least two distinct carboxylate side chains (Shoshan & Selman, 1980; Arana & Vallejos, 1980, 1981).

In a previous study (Sharp & Frasch, 1985), we have shown that proton spin-echo NMR provides an effective means of observing selectively small subsets of amino acids which have atypically high reorientational mobility. This study was concerned primarily with a number of relatively narrow resonances with 1–10-Hz line widths which persist in the 18-ms spin-echo spectrum. This residual spectrum is comprised of 0.4% of the total proton intensity (approximately 20 amino acids) and arises from one or more highly charged random-coil peptide segments which extend into the aqueous environment.

In this study, we investigate the influence of substrate binding on the 18-ms SE spectrum of CF_1. For this purpose, we have used 5′-adenylyl β-imidodiphosphate (AMPPNP), which is a nonhydrolyzable analogue of ATP. In the presence of Mg^{2+}, AMPPNP binds tightly to CF_1 ($K_d \approx 7$ μM) as well as to the mitochondrial coupling factor F_1. Reported stoichiometries of binding for the two coupling factors are 2 and 3 mol of analogue per mole of enzyme, respectively (Cantley & Hammes, 1975; Cross & Nalin, 1982). AMPPNP is a competitive inhibitor of the ATPase activity of both enzymes. In the present experiments, the binding of Mg·AMPPNP to CF_1 produced specific immobilization of the NMR-visible asparate and glutamate side chains. Mangano-AMPPNP was found to have a more pronounced effect on these same side chains. Because Mn^{2+} is a paramagnetic ion with an electronic spin of $^5/_2$, this ion affects nearby proton resonances in the SE spectrum not only by alterations in mobility due to binding but also as a result of paramagnetic relaxation. In particular, the paramagnetic dipole–dipole interaction provides a through-space magnetic coupling which is highly distance dependent ($T_2^{-1} \sim r^{-6}$) with an effective range of approximately 20 Å. Thus, a comparison of the effects of Mn·AMPPNP and Mg·AMPPNP complexes on the spin-echo spectrum of CF_1 provided information concerning the proximity of specific proton resonances to the metal ion binding site.

Materials and Methods

Coupling factor 1 was isolated from spinach, purified by using DEAE-Sephadex column chromatography and high-performance liquid chromatography, and stored as ammonium sulfate precipitates. NMR samples contained typically 10 mg of protein in 0.6 mL of deuterated borate buffer (99.96% D_2O, pH* 9.0). Details of the preparative procedure and sample preparation are the same as those given elsewhere (Sharp & Frasch, 1985) except for presence of 50 mM NaCl in the final NMR sample.

5′-Adenylyl β-imidodiphosphate (Sigma) was prepared as a 20 mM stock solution in the deuterated borate buffer. Samples were incubated for 45 min at 37 °C prior to measurement to permit equilibration of binding (Cross & Nalin, 1982). NMR measurements were conducted at 360 MHz and 37 °C using a Bruker WM-360 spectrometer as previously described (Sharp & Frasch, 1985).

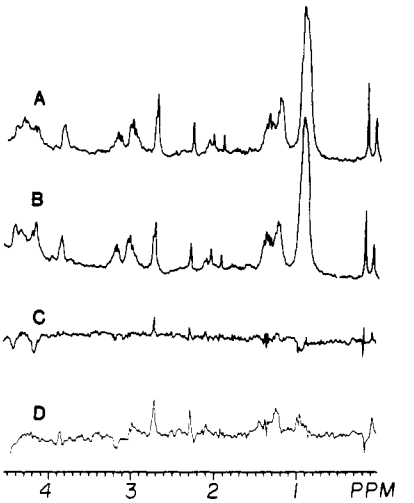

FIGURE 1: High-field portion of the 18-ms proton spin-echo spectrum of DTT-activated CF_1 at 37 °C before (A) and after (B) addition of 3 mol of Mg·AMPPNP. Spectrum C is the difference spectrum (A) − (B). (D) is the spin-echo difference spectrum of CF_1 formed ±3 mol of Mn·AMPPNP per mole of CF_1. Spectra comprise 1500 transients of 8K data points.

Results

The upfield portion of the 360-MHz proton spin-echo NMR spectrum of CF_1 obtained at an interpulse spacing of 18 ms is shown in Figure 1A. Specific characteristics of this spectrum and the identity of the contributing amino acid side chains have been discussed previously (Sharp & Frasch, 1985). A second spin-echo spectrum was accumulated after addition of the substrate analogue Mg·AMPPNP to the protein in a 3:1 molar stoichiometry (Figure 1B). Changes in the spectrum are subtle and specific and are best visualized in the spin-echo difference spectrum formed by subtracting the +Mg·AMPPNP spectrum from the −Mg·AMPPNP spectrum (Figure 1C). The two negative peaks at 4.1 and 4.4 ppm are due to ribose protons on the added AMPPNP. Among the protein resonances, appreciable perturbations are seen in the peaks at 2.70 and 2.29 ppm, which we have previously assigned to aspartate β-CH_2 and glutamate γ-CH_2 resonances, respectively (Sharp & Frasch, 1985). These assignments are based on chemical shift values and on the selective immobilization that is produced in these resonances following treatment with Woodward's reagent K, a specific covalent modifying agent for carboxyls. The positive difference peaks in Figure 1C represent a specific relaxation enhancement due to immobilization of these two resonances upon binding of Mg·AMPPNP.

Spectral perturbations are also apparent in the methyl proton region, between 0.0 and 1.3 ppm. Significant relaxation enhancements occur in the multiplet at 1.25 ppm (possibly a theonine methyl), as well as in the two upfield singlets near 0.1 ppm, for which the assignments are not well established. The aliphatic methyl peaks near 0.9–1.0 ppm show relatively little perturbation upon nucleotide binding.

Spin-echo spectra obtained at an interpulse spacing of 18 ms were recorded for solutions of CF_1 following serial additions of Mg·AMPPNP at ratios of 1, 2, 3, 5, and 7 mol of analogue per mole of CF_1. A series of difference spectra were formed by subtracting the spectrum obtained in the presence of analogue from the no-additions spectrum. Pronounced negative peaks appeared at 6.17, 4.41, and 4.19 ppm due to ribose protons on AMPPNP which is free in solution; protons from

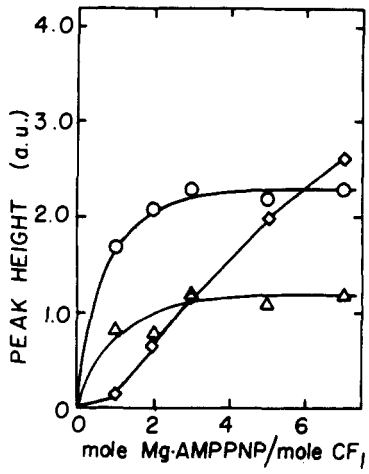

FIGURE 2: Plots of peak heights in the 18-ms spin-echo difference spectra of CF_1 formed ± added Mg·AMPPNP. Curves correspond to the ribose resonance at 6.17 ppm (diamonds), the aspartate methylene resonance at 2.70 ppm (circles), and the glutamate methylene resonance at 2.35 ppm (triangles).

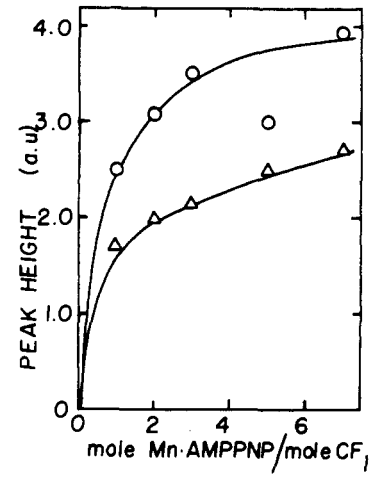

FIGURE 3: Plots of peak heights in the 18-ms difference spectra of CF_1 formed ± added Mn·AMPPNP. Curves correspond to the aspartate resonance at 2.70 ppm (circles) and the glutamate methylene resonance at 2.35 ppm (triangles).

the bound form of AMPPNP are strongly broadened and are not detectable as resolved peaks. A plot of the peak amplitude of the ribose H1′ resonance (6.17 ppm) as a function of added nucleotide (Figure 2) indicates that only the first molar equivalent of Mg·AMPPNP was bound tightly to the enzyme. The binding stoichiometry was approximately 1 mol of AMPPNP per mole of CF_1.

Figure 2 also contains plots of the peak amplitude of the assigned glutamate and aspartate resonances from the SED spectra as a function of added nucleotide. The plots show that the immobilization of these side chains is caused by the tight binding of metal–nucleotide to the enzyme. The stoichiometry of binding is approximately 1 mol of nucleotide per mole of CF_1, and the K_d is in the low micromolar range. The solid lines in Figure 2 were calculated by assuming a single binding site with a K_d of 1 μM.

Quantitation of the difference peaks is difficult, but we estimate that for the stoichiometrically bound enzyme the total intensity loss is approximately one proton per CF_1 for the peak at 2.71 ppm and approximately 0.5 proton per CF_1 for the peak at 2.29 ppm. Thus, the intensity of these two difference peaks corresponds to approximately half the total intensity of the parent peaks. The fact that the immobilization reaches a maximum without entirely eliminating the peaks at 2.71 and 2.29 ppm probably indicates that these side chains are involved in a rapid equilibrium between free and bound environments such that the average T_2 is shortened. In this situation, a small population of bound side chains could produce the observed relaxation enhancement.

The effect of the binding of Mn·AMPPNP on the 18-ms spin-echo spectrum of CF_1 is shown in Figures 1D and 3. Ribose peaks are absent in these spectra due to the association of Mn(II) with the free nucleotide. As was observed in difference spectra produced by the magnesium complex, the addition of Mn·AMPPNP specifically shortened the T_2 of the methylene resonances at 2.71 and 2.29 ppm, as well as the resonance near 1.25 ppm. The resonance at 2.29 ppm also exhibited an upfield shift. The stoichiometry of binding, as measured by the two methylene peaks, remained near 1 mol per mole of CF_1 (Figure 3). The major relaxation enhancement clearly resulted from the tightly bound nucleotide, while a much smaller nonspecific effect observed at high mole ratios of nucleotide to CF_1 is also evident due to Mn·AMPPNP in free solution.

The relaxation enhancement produced by Mn·AMPPNP was about twice as large as that produced by the magnesium complex. If the two complexes bind isostructurally to CF_1, this result suggests that the additional relaxation enhancements arise from through-space nuclear–electron dipolar couplings to bound Mn(II). Since the effective range of this interaction is approximately 20 Å (see Discussion), it is probable that the protons responsible for the difference peaks at 2.71 and 2.29 ppm result from protons which lie within this dipolar sphere of influence. However, these peaks were only partially eliminated from the 18-ms spin-echo spectrum when the metal–nucleotide complex was bound. This indicates that these side chains are not directly coordinated to the metal ion but rather lie in the periphery of the dipolar sphere of influence.

In contrast, resonances in the spin-echo spectrum that were not significantly broadened by Mn·AMPPNP must lie outside the dipolar sphere of influence. This group includes the lysine ϵ-CH_2 resonance, which gives rise to a small, sigmoidal difference peak near 3.0 ppm, and the aliphatic methyl peaks near 0.9 ppm, which exhibit sigmoidal character with little net intensity perturbation. The difference spectra formed ±Mn·AMPPNP also contain one pronounced negative peak at 3.2 ppm. The assignment of this peak is not certain, although reference chemical shifts of random-coil peptides suggest that it may arise from an arginine δ-CH_2 resonance. The observation of a marked negative difference peak is somewhat surprising in that it corresponds to a lengthening, rather than a shortening, of T_2 in the Mn-containing enzyme. Evidently this resonance, which experiences increased mobility due to the binding of Mn·AMPPNP, also lies outside the sphere of significant paramagnetic dipolar relaxation.

Discussion

The major features of the 18-ms spin-echo spectrum are discussed in an earlier paper (Sharp & Frasch, 1985). The experiments presented here investigated the effect of stoichiometric concentrations of added AMPPNP, a nonhydrolyzable substrate analogue, on the spin-echo spectrum of CF_1. Difference spin-echo spectra obtained ±Mg·AMPPNP and ±Mn·AMPPNP were recorded to detect perturbations of specific amino acids involved in ligand binding. Specific relaxation enhancements were observed in two methylene peaks assigned to aspartate (β-CH_2) and glutamate (γ-CH_2) after addition of the substrate analogue Mg·AMPPNP in a range near 1 mol of Mg·AMPPNP per mole of CF_1. The concen-

tration dependence of the relaxation enhancements indicates that they result from the binding of Mg·AMPPNP to a single tight site, for which the K_d is in the low micromolar range. Under somewhat different experimental conditions, AMPPNP has been observed to bind to the active sites both of CF_1 (Cantley & Hammes, 1975) and of the mitochondrial F_1 (Cross & Nalin, 1981) with similar binding constants. Cantley & Hammes (1975) concluded that latent CF_1 contains two tight binding sites for Ca·AMPPNP. They further found that heat activation of the enzyme produces a third nucleotide binding site, which can be occupied by Ca·AMPPNP but not by Ca·ADP. The relaxation enhancements observed in the present work using protein activated by dithiothreitol clearly result from Mg–nucleotide complex binding to a single tight site. Binding is saturated at 1 mol of added nucleotide per mole of CF_1, indicating that this site has the lowest binding constant of any accessible nucleotide binding site on the enzyme. Further work is needed to clarify the relation between the binding site visible by NMR and those inferred by other workers.

In order to provide a measure of the distance of NMR-visible protons from the metal ion binding site, we have compared spectral changes produced by Mg·AMPPNP with those produced by Mn·AMPPNP. Mn(II) is a paramagnetic $S = {}^5/_2$ ion, which provides a highly efficient relaxation pathway for neighboring protons. Paramagnetic T_2 contributions are produced additively (1) by through-space magnetic dipole coupling between the paramagnetic spin of Mn(II) and resonant protons and (2) by scalar interactions, which are propagated by spin polarization through chemical bonds. Both of these interactions are of inherently limited range. The scalar interaction is rarely significant beyond four to five bonds except in conjugated systems. The dipolar contribution falls off as r^{-6}, where r is the distance from the paramagnetic center to the resonant proton. An estimate of the range of the paramagnetic interaction has been made by using the Solomon–Bloembergen–Morgan theory (Solomon & Bloembergen, 1955; Dwek, 1973) and indicates that an observable paramagnetic effect (i.e., an enhancement $\geq 10\ s^{-1}$ in T_2^{-1}) will be produced for protons within 18–24 Å of bound Mn(II).[2]

The data of Figures 2 and 3 suggest that the carboxyl-bearing side chains observed at 2.71 and 2.29 ppm are specifically immobilized upon nucleotide binding and that the site of immobilization lies within the dipolar sphere of influence of the paramagnetic center. However, it is unlikely that the carboxyl side chains coordinate directly to the metal chain. Such binding would lead to large relaxation enhancements of the adjacent methylene protons, thereby removing these resonances from the difference spectrum. Direct coordination to the metal ion would also be expected to bring neighboring amino acid resonances, for example, those due to the methine backbone protons, well into the sphere of efficient paramagnetic relaxation. Large relaxation enhancements are not, in fact, observed for other protons along the chain. Thus, the majority of the NMR-visible amino acids remain outside the dipolar sphere of influence of bound Mn(II). From the magnitude of the observed relaxation enhancements, it appears that the site of immobilization of the side-chain carboxyls lies in the outer regions of this sphere approximately 15–20 Å from the metal.

These results are consistent with previous observations (Arana & Vallehos, 1981) concerning the inactivation of enzymatic activity produced by covalent modification of carboxyl groups on CF_1 with WRK. This reagent, which affects the aspartate and glutamate side chains that contribute to the SE spectrum, does not react with the DCCD-modifiable glutamate-204 of the β subunit (Esch et al., 1981). Glutamate-204 lies in the middle of the sequence of the β subunit and is protected from DCCD modification by divalent metals. This suggests that Glu-204 is involved with metal ion binding at the active site. However, the WRK-modifiable carboxyls are not protected by divalent metals but instead by nucleotides (Arana & Vallehos, 1981). The stereospecificity of the substrate for the active site of CF_1 has been determined both for the phosphato–metal complex that is formed (Frasch & Selman, 1981) and also for the ribose of the nucleotide (Schlimme et al., 1979). The stereoconfiguration of the metal–nucleotide complex when bound to the active site is such that the distal point of the adenine ring (the C6 amino group) is about 14 Å from the divalent metal. A carboxyl group interacting with the adenine moiety of the substrate could be as much as 15–20 Å away from the divalent metal.

We have also recorded difference spectra at shorter spin-echo pulse spacings, where intensity from other, less mobile amino acids contributes to the spectrum. Rather dramatic changes in mobility have been observed in these spectra, although the peaks are less well resolved and are consequently more difficult to interpret. A preliminary account of these results is given elsewhere (Sharp & Frasch, 1985).

Registry No. Mg·AMPPNP, 69977-25-9; Mn·AMPPNP, 61994-37-4; ATP synthase, 37205-63-3; L-aspartic acid, 56-84-8; L-glutamic acid, 56-86-0.

[2] These limits correspond to limiting values of τ_c, the correlation time of the paramagnetic center. A lower limit to τ_c is set by the reorientational correlation time of CF_1 ($\approx 10^{-7}$ s). An upper limit to τ_c is determined by the position of the relaxation maximum in the field dispersion profile of the solvent proton T_1 (Dwek, 1973). This maximum occurs near 0.5 T (unpublished results), placing τ_c in the range 0.5×10^{-8} to 1.0×10^{-7} s at 8.4 T.

References

Andreo, C. S., & Vallejos, R. H. (1977) *FEBS Lett. 78*, 207–210.

Arana, J. L., & Vallejos, R. H. (1980) *FEBS Lett. 113*, 319–322.

Arana, J. L., & Vallejos, R. H. (1981) *FEBS Lett. 123*, 103–106.

Boyer, P. D. (1980) in *Membrane Bioenergetics* (Lee, C. P., et al., Eds.) pp 461–479, Addison-Wesley, Palo Alto, CA.

Cantley, L. C., & Hammes, G. G. (1975) *Biochemistry 14*, 2968–2975.

Carlier, M.-F., Holowka, D. A., & Hammes, G. G. (1979) *Biochemistry 18*, 3452–3457.

Cross, R. L., & Nalin, C. M. (1982) *J. Biol. Chem. 257*, 2874–2881.

Deters, D. W., Racker, E., Nelson, N., & Nelson, H. (1975) *J. Biol. Chem. 250*, 1041–1047.

Dunn, S. D., & Hepple, L. A. (1981) *Arch. Biochem. Biophys. 210*, 421–436.

Dwek, R. A. (1973) *N.M.R. in Biochemistry*, Chapter 9, Clarendon Press, Oxford.

Esch, F. S., Bohlen, P., Otsuka, A. S., Yoshida, M., & Allison, W. S. (1981) *J. Biol. Chem. 256*, 9084–9089.

Frasch, W. D., & Selman, B. R. (1981) *Biochemistry 20*, 3636–3643.

Frasch, W. D., & Sharp, R. R. (1984) *Adv. Photosynth. Res. 2*, 591–594.

Merchant, S., Shaner, S. L., & Selman, B. R. (1983) *J. Biol. Chem. 258*, 1026–1031.

Moroney, J. V., Lopresti, L., McEwen, B. F., McCarty, R. E., & Hammes, G. G. (1983) *FEBS Lett. 158*, 58–62.

Oliver, D., & Jagendorf, A. (1976) *J. Biol. Chem. 251*, 7168-7175.
Penefsky, H. S. (1979) *Adv. Enzymol. Relat. Areas Mol. Biol. 49*, 111-138.
Schlimme, E., de Groot, E. J., Schott, E., Strottman, H., & Edelmann, K. (1979) *FEBS Lett. 106*, 251-256.
Schmid, R., Jagendorf, A. R., & Hulkower, S. (1977) *Biochim. Biophys. Acta 462*, 177-186.
Sharp, R. R., & Yocum, C. F. (1980) *Biochim. Biophys. Acta 592*, 185-195.
Sharp, R. R., & Frasch, W. D. (1985) *Biochemistry* (preceding paper in this issue).
Shoshan, V., & Selman, B. R. (1980) *J. Biol. Chem. 255*, 384-389.
Solomon, I., & Bloembergen, N. (1956) *J. Chem. Phys. 25*, 261.
Sugayama, Y., & Mukohata, Y. (1978) *FEBS Lett. 85*, 211-214.
Sugayama, Y., & Mukohata, Y. (1979) *FEBS Lett. 98*, 276-280.
Vallejos, R. (1981) in *Energy Coupling in Photosynthesis* (Selman & Selman, Eds.) Elsevier/North-Holland, Amsterdam.
Vallejos, R. H., Viale, A. M., & Andreo, C. S. (1977) *FEBS Lett. 84*, 304-308.
Webb, M. R., Grubmeyer, C., Penefsky, H. S., & Trentham, D. R. (1980) *J. Biol. Chem. 255*, 11637-11639.

Effect of pH on the Conformation of Diphtheria Toxin and Its Implications for Membrane Penetration†

Michael G. Blewitt, Laura A. Chung, and Erwin London*
Department of Biochemistry, State University of New York at Stony Brook, Stony Brook, New York 11794-5215
Received October 25, 1984

ABSTRACT: The pH-triggered change in diphtheria toxin conformation and the physical properties of the toxin above and below the transition pH have been examined. Exposure to low pH (≤5 at 23 °C, ≤5.3 at 37 °C) triggers a rapid ($t_{1/2}$ < 30 s) change in toxin conformation; the transition occurs over a narrow pH range (0.2 unit). Below the transition pH, buried tryptophans become exposed, and the toxin becomes hydrophobic, binding very tightly to detergent. Aggregation is observed at low pH, probably due to this extreme hydrophobicity. Circular dichroism and fluorescence properties show that the low-pH conformation is not extensively unfolded. Therefore, the toxin "opens" at low pH without becoming a random coil. The conformation change is partly irreversible, and the degree of irreversibility parallels the degree of aggregation. Reduction of the disulfide bonds does not increase hydrophobicity at neutral pH. Furthermore, none of the structural variants of toxin (monomer or dimer, bound to ApUp or free, and nicked between subunits or intact) are hydrophobic at neutral pH or differ in transition pH markedly. Therefore, these factors do not mimic the effect of low pH. These observations are consistent with a functional role for the pH-triggered changes during penetration of the membranes of acidic organelles. The toxin may have adapted a conformational change similar to partial denaturation for a critical role in function. The possible nature of the pH-sensitive interactions and the effects of aggregation are discussed briefly.

Diphtheria toxin is a protein (M_r 58 340) that kills cells by inhibition of protein synthesis. It is composed of two domains: subunit A which inactivates elongation factor 2 by ADP-ribosylation, and subunit B which binds to a receptor molecule and also is required to translocate subunit A into the cytoplasm. The structure of the toxin at neutral pH and its enzymatic function have been extensively studied (Collier, 1983; Pappenheimer, 1977; Uchida, 1983). The sequence of each subunit is now known (Greenfield et al., 1983; Kaczorek et al., 1983; Ratti et al., 1983). Several studies indicate that the toxin enters cells by receptor-mediated endocytosis, followed by penetration through the membrane of an acidic organelle (Draper & Simon, 1980; Sandvig & Olsnes, 1980, 1981). Indirect evidence suggests that acidic endosomes are the most likely site of membrane penetration (Marnell et al., 1984). The importance of low pH in membrane penetration by toxin is demonstrated both by the ability of lysosomotropic amines, which increase pH in acidic organelles, to inhibit toxicity and from the ability of low-pH incubation of cells with surface-bound toxin to overcome this block (Sandvig & Olsnes, 1980, 1981). Furthermore, such a low-pH incubation with surface-bound toxin can restore toxicity when endocytosis is blocked at low temperatures (Draper & Simon, 1980). In model systems, low-pH induction of toxin hydrophobicity (Blewitt et al., 1984; Sandvig & Olsnes, 1981) and low-pH-induced pore formation in membranes (Donovan et al., 1981; Kagan et al., 1981; Misler, 1983, 1984) have been observed. However, these studies have not yet explained the exact mechanisms of membrane penetration and of subunit A translocation.

In previous preliminary studies, we have noted a distinct change in toxin conformation at low pH (Blewitt et al., 1984; London et al., 1984). In this report, the conformational change at the pH transition has been further characterized, as well

† This work was supported by National Institutes of Health Grant GM31986 and by a University Award and a Biomedical Research Grant from the State University of New York to E.L.

0006-2960/85/0424-5458$01.50/0